

Forward Kinematics of Object Transport by a Multi-Robot System with Deformable Sheet

Jiawei Hu, Wenhang Liu, Jingang Yi and Zhenhua Xiong

Abstract—We present object handling and transport by a multi-robot team with a deformable sheet as a carrier. Due to the deformability of the sheet and the high dimension of the whole system, it is challenging to clearly describe all the possible positions of the object on the sheet for a given formation of the multi-robot system. A complete forward kinematics (FK) method is proposed in this paper for object handling by an N -mobile robot team with a deformable sheet. Based on the virtual variable cables model, a constrained quadratic problem (CQP) is formulated by combining the form closure and minimum potential energy conditions of the system. Analytical solutions to the CQP are presented and then further verified with the force closure condition. With the proposed FK method, all possible solutions are obtained with the given initial sheet shape and the robot team formation. We demonstrate the effectiveness, completeness, and efficiency of the FK method with simulation and experimental results.

Index Terms—Object handling and transport, multi-robot system, forward kinematics, deformable sheet

I. INTRODUCTION

As a common handling carrier, a deformable sheet can be easily used to hold the object steadily, while the operators can apply force to hold the sheet at multiple locations. For example, rectangular bed sheets are often used in hospitals when transferring patients, where multiple persons hold the sheet at corners [1]. Instead of human operators, mobile robots are used to hold the deformable sheet to handle and transport objects [2]. Due to the highly deformable sheet [3], robotic manipulation of the sheet is a challenging problem [4]. A simplified model of the deformable sheet and multi-robot manipulation of deformable objects have been used in [5], [6]. Hunte and Yi [2] proposed a sheet-handling system using three mobile robots that held and supported the sheet vertices. In [7], a geometric link model of the sheet-object kinematic relationship was proposed for a three-robot team to transport an object to follow a given trajectory. The recent work in [8] further extended the sheet-object kinematic model to include the rotational motion of a spherical-shaped object for pose manipulation. However, these work only considered three mobile robots and as the number of robots increases, the

transported object may have multiple equilibrium states on the sheet and the above-mentioned results cannot be directly applied.

Inspired by the cable suspended robots (CSRs) [9], the virtual variable cables model (VVCN) was proposed in [10], and by using VVCN, the robots-sheet-object interactions can be viewed as a robot-cable-object system. The effectiveness of the VVCN approach was verified through simulations and object transporting experiments. In order to maintain the stability of the object during the handling process, all virtual cables were assumed to be straight and taut. As the cable in CSRs can be slack [11], the virtual cable in the VVCN therefore has a slack state. With different numbers of taut cables under the same robot formation, the transported object may have multiple equilibrium states. The object position at each equilibrium state is obtained by the forward kinematics (FK) method for the multi-robot system. As the number of robots increases, the number of combinations of possible taut cable configurations exponentially increases and not all combinations are valid FK solutions. Therefore, it is a challenging task to effectively and efficiently determine the equilibrium states of the multi-robot system for object transport.

The concept of taut cable in VVCN corresponds to the positive cable tension in the field of CSRs [12] and cable-driven parallel robots (CDPRs) [13]. Inspired by the modeling method of CSRs and CDPRs, we obtain three conditions that need to be satisfied to solve the FK problem of VVCN. The first condition is the form closure condition that satisfies the geometric constraints of the cable length [14]. For CSRs and CDPRs, the length of the cable can be actively controlled [15], [16] or be fixed, and the object was manipulated by changing the robotic formation [17]. These configurations are different from VVCN, in which the length of the cable is constrained by the initial shape of the sheet. The second condition is the minimum potential energy of the system under the quasi-static condition [18]. We obtain the free energy of the robots-sheet-object system based on [2], and construct a constrained quadratic problem (CQP) combined with geometric constraints. The third condition is to satisfy the force closure condition [19] and the tension of the cable should be non-negative [20].

Based on the above three conditions, we propose a novel FK method of multi-robot system with a deformable sheet. The FK method obtains all valid solutions with possible taut cable combinations. We first transform the geometric constraints from quadratic equations into linear equations, and the form closure condition is checked by the rank of the augmented matrix. The CQP is proposed by combining the

This work was supported in part by the National Natural Science Foundation of China (U1813224). The code of the proposed Forward Kinematics method is publicly available at https://github.com/sjtuhjw/VVCN_FK. (Corresponding author: Zhenhua Xiong, Jingang Yi).

Jiawei Hu, Wenhang Liu and Zhenhua Xiong are with the School of Mechanical Engineering, Shanghai Jiao Tong University, Shanghai, China. (e-mail: hu_jiawei@sjtu.edu.cn; liuwenhang@sjtu.edu.cn; mexiong@sjtu.edu.cn).

J. Yi is with the Department of Mechanical and Aerospace Engineering, Rutgers University, Piscataway, NJ 08854 USA. (e-mail: jgyi@rutgers.edu).

form closure condition and minimum potential energy of the system. In order to obtain a general solution for CQP, the Lagrange multiplier method (e.g., [21]) is adopted and the force closure condition is checked to obtain physically feasible solutions. The effectiveness of the method and the algorithm is verified through a four-robot experiment and the completeness of the FK method is verified through simulation. The main contribution of this paper is the novel computational forward kinematics method and algorithm of a multi-robot system with a deformable sheet. The proposed FK algorithms can be further extended for real-time multi-robot control for object handling and transporting with a deformable sheet.

The remainder of this paper is organized as follows. The system configuration and the problem statement are given in Section II. In Section III, the complete FK method and algorithm are proposed. Simulation and experimental results are presented in Section IV. Finally, Section V summarizes the concluding remarks.

II. SYSTEM CONFIGURATION AND PROBLEM STATEMENT

We consider that N mobile robots hold a deformable sheet to handle and transport an object. Fig. 1(a) illustrates the basic configuration of the robotic system. A team of N mobile robot, $N \geq 3, N \in \mathbb{N}$, holds a flexible sheet \mathcal{S} at points $\mathbf{p}_i, i = 1, \dots, N$, and object O is sit on \mathcal{S} . An inertial coordinate system \mathcal{W} is setup with the Z -axis upward. The planar position of each robot is denoted as $\mathbf{r}_i = [x_i \ y_i]^T, i = 1, \dots, N$ in \mathcal{W} . The robot formation is denoted as $\mathcal{R}_N = [\mathbf{r}_1 \ \dots \ \mathbf{r}_N]^T \in \mathbb{R}^{N \times 2}$. The position of the robot-sheet holding point is denoted as $\mathbf{p}_i = [\mathbf{r}_i^T \ z_r]^T$, where z_r is the a constant height for all holding points, as shown in Fig. 2.

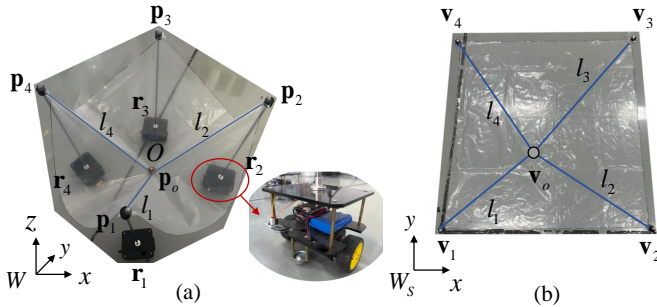


Fig. 1. The system configuration and experimental setup for a four-robot team. (a) Experimental setup and system configuration. Positions of the robot \mathbf{r}_i , the holding point \mathbf{p}_i and the object \mathbf{p}_o in the world coordinate system \mathcal{W} . (b) The initial shape of the deformable sheet in the local coordinate system \mathcal{W}_S . Virtual cables l_i is determined by the contact point \mathbf{v}_o .

For sheet \mathcal{S} , the initial shape is a convex polygon with N vertices in the local planar frame \mathcal{W}_S attached to the sheet, as shown in Fig. 1(b). The initial position vector of the vertices in \mathcal{W}_S is denoted as $\mathcal{V}_N^0 = [\mathbf{v}_1 \ \dots \ \mathbf{v}_N]^T \in \mathbb{R}^{N \times 2}$, where the i th vertex's position in \mathcal{W}_S is $\mathbf{v}_i = [x_{vi} \ y_{vi}]^T, i = 1, \dots, N$. The contact point between object O and the sheet is denoted as $\mathbf{v}_o = [x_{vo} \ y_{vo}]^T$ in \mathcal{W}_S . The premise of the convex polygonal sheet ensures that the line between \mathbf{v}_o and \mathbf{v}_i exists and can be viewed as the virtual cable in VVCM.

Object O is considered as a point mass and the motion of the object is quasi-static, that is, the dynamic effects of

the particular motion are neglected. Moreover, the deformable sheet is assumed to be inelastic and soft. Based on these assumptions, the object moves freely on the sheet under the gravitational force and stays at the position where the system energy is minimal. The convex N polygon sheet is viewed as N virtual cables by VVCM, and the length of each cable is denoted as $l_i = \|\mathbf{v}_i - \mathbf{v}_o\|_2, i = 1, \dots, N$. When \mathbf{v}_o changes, virtual cables vary. Since the virtual cables might be taut or slack, as shown in Fig. 1(c), the Euclidean distance between \mathbf{p}_o and \mathbf{p}_i in \mathcal{W} is less than or equal to the corresponding virtual cable length l_i in \mathcal{W}_S , that is,

$$l_i = \|\mathbf{v}_i - \mathbf{v}_o\|_2 \geq \|\mathbf{p}_i - \mathbf{p}_o\|_2, i = 1, \dots, N. \quad (1)$$

Let \mathcal{I}_t denote the index set of all taut cables and its cardinality is denoted as $k = |\mathcal{I}_t|$. Because the sheet is inelastic and completely flexible, it is obvious that $3 \leq k \leq N$. Fig. 2 illustrates an example of three possible combinations of taut/slack virtual cables of a 5-robot team under the same formation to hold object O by a deformable sheet, that is, $\mathcal{I}_t = \{1, 2, 3, 4, 5\}, \mathcal{I}_t = \{1, 2, 3, 4\}$, and $\mathcal{I}_t = \{1, 2, 4\}$ with $k = 5, 4, 3$, respectively. This example illustrates that different \mathcal{I}_t under the same robot formation can lead to different equilibrium states for object O .

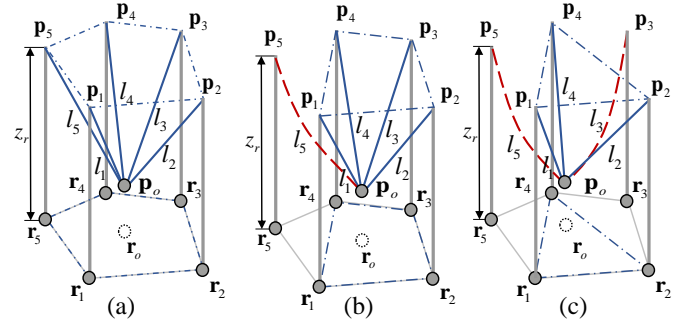


Fig. 2. Three possible static equilibrium conditions for a five-robot formation. (a) $\mathcal{I}_t = \{1, 2, 3, 4, 5\}$ and $k = |\mathcal{I}_t| = 5$. (b) $\mathcal{I}_t = \{1, 2, 3, 4\}$ and $k = |\mathcal{I}_t| = 4$. (c) $\mathcal{I}_t = \{1, 2, 4\}$ and $k = |\mathcal{I}_t| = 3$.

Problem Statement: For the N -robot system with a deformable sheet \mathcal{S} to hold object O , the goal of the forward kinematics problem is to find all possible object position \mathbf{p}_o in \mathcal{W} and corresponding \mathbf{v}_o in \mathcal{W}_S under given a robot formation \mathcal{R}_N (i.e., $\mathbf{p}_i, i = 1, \dots, N$).

From the above statement, the output of each FK solution consists of *five variables* ($\mathbf{p}_o, \mathbf{v}_o$), $\mathbf{p}_o \in \mathbb{R}^3$ and $\mathbf{v}_o \in \mathbb{R}^2$ along with taut cable set \mathcal{I}_t . Since there exist multiple equilibria under a given \mathcal{R}_N , all FK solutions then include the object position set $\mathbb{P}_o = \{\mathbf{p}_o\}$ and the corresponding sheet position set $\mathbb{V}_o = \{\mathbf{v}_o\}$. The taut cable set group $\mathbb{I}_t = \{\mathcal{I}_t\}$.

III. FORWARD KINEMATICS METHODS AND ALGORITHM

For a possible FK solution, it should satisfy the form closure condition, minimum potential energy condition, and force closure condition simultaneously.

A. Forward Kinematics Methods

1) *Form Closure Condition:* Without loss of generality, we denote the taut cable set $\mathcal{I}_t = \{i_1, i_2, \dots, i_k\}$, and the slack

cable index set is then $\mathcal{I}_s = \mathcal{I}_N \setminus \mathcal{I}_t = \{i_{k+1}, i_{k+2}, \dots, i_N\}$, where \mathcal{I}_N is the entire index set of \mathcal{R}_N . In each element in \mathcal{I}_t , the inequality in (1) becomes equality, namely, the form closure condition satisfies the following geometric constraint.

$$\|v_i - v_o\|_2^2 = \|r_i - r_o\|_2^2 + (z_r - z_o)^2, \quad i \in \mathcal{I}_t \quad (2)$$

Since $v_o \in \mathbb{R}^3$, at least three geometric constraints are required to satisfy (2), i.e., $k \geq 3$. With the given \mathcal{R}_N , the geometric constraints (1) are expressed as the following N formulas.

$$z_o = z_r - [(x_{vi_1} - x_{vo})^2 + (y_{vi_1} - y_{vo})^2 - (x_{i_1} - x_o)^2 - (y_{i_1} - y_o)^2]^{\frac{1}{2}}, \quad (3a)$$

$$b_i = (x_i - x_{i_1})x_o + (y_i - y_{i_1})y_o - (x_{vi} - x_{vi_1})x_{vo} - (y_{vi} - y_{vi_1})y_{vo}, \quad i \in \mathcal{I}_t, i \neq i_1 \quad (3b)$$

$$b_i < (x_i - x_{i_1})x_o + (y_i - y_{i_1})y_o - (x_{vi} - x_{vi_1})x_{vo} - (y_{vi} - y_{vi_1})y_{vo}, \quad i \in \mathcal{I}_s \quad (3c)$$

where $b_i = \frac{x_{vi_1}^2 + y_{vi_1}^2 - x_{i_1}^2 - y_{i_1}^2}{2} - \frac{x_{vi}^2 + y_{vi}^2 - x_i^2 - y_i^2}{2}$. (3a) can be directly obtained by plugging $i = i_1$ into (2), which is a quadratic equation with respect to all five output variables (p_o, v_o) . The rest $(N - 1)$ formulas in (3b) and (3c) are obtained by subtracting (2) from (1), which are linear with $x = [x_o \ y_o \ x_{vo} \ y_{vo}]^T \in \mathbb{R}^4$ and can be rewritten as

$$\mathbf{A}_1 \mathbf{x} = \mathbf{b}_1, \quad \mathbf{A}_2 \mathbf{x} > \mathbf{b}_2. \quad (4)$$

where $\mathbf{A}_1 \in \mathbb{R}^{(k-1) \times 4}$, $\mathbf{A}_2 \in \mathbb{R}^{(N-k) \times 4}$, $\mathbf{b}_1 \in \mathbb{R}^{(k-1)}$, $\mathbf{b}_2 \in \mathbb{R}^{(N-k)}$, which can be expressed as follows

$$\mathbf{A}_1 = \begin{bmatrix} x_{i_2} - x_{i_1} & y_{i_2} - y_{i_1} & x_{vi_1} - x_{vi_2} & y_{vi_1} - y_{vi_2} \\ \vdots & \vdots & \vdots & \vdots \\ x_{i_k} - x_{i_1} & y_{i_k} - y_{i_1} & x_{vi_1} - x_{vi_k} & y_{vi_1} - y_{vi_k} \end{bmatrix}$$

$$\mathbf{A}_2 = \begin{bmatrix} x_{i_{k+1}} - x_{i_1} & y_{i_{k+1}} - y_{i_1} & x_{vi_1} - x_{vi_{k+1}} & y_{vi_1} - y_{vi_{k+1}} \\ \vdots & \vdots & \vdots & \vdots \\ x_{i_N} - x_{i_1} & y_{i_N} - y_{i_1} & x_{vi_1} - x_{vi_N} & y_{vi_1} - y_{vi_N} \end{bmatrix}$$

$$\mathbf{b}_1 = [b_{i_2} \ \dots \ b_{i_k}]^T, \text{ and } \mathbf{b}_2 = [b_{i_{k+1}} \ \dots \ b_{i_N}]^T.$$

When \mathbf{x} is solved and the object height z_o is obtained by (3a), the solution to the FK problem is then obtained. Therefore, we now focus on solving and obtaining \mathbf{x} .

From the above discussion, the form closure condition can be simplified as whether the solution of $\mathbf{A}_1 \mathbf{x} = \mathbf{b}_1$ exists. Defining augmented matrix $\bar{\mathbf{A}}_1 = [\mathbf{A}_1 \ \mathbf{b}_1] \in \mathbb{R}^{(k-1) \times 5}$, the necessary condition for (4) to have the solution is given as

$$\text{rank}(\mathbf{A}_1) = \text{rank}(\bar{\mathbf{A}}_1), \quad (5)$$

where rank represents the rank of a matrix. The computational complexity for determining condition (5) is $O(k^2)$ at worst case. The taut cable sets that do not meet the condition can be directly eliminated and therefore, this condition greatly saves the amount of subsequent computations.

2) *Minimum Potential Energy*: We need to find the minimum potential energy condition of the system to solve \mathbf{x} in each equilibrium state. Considering the gravitational force of the object on sheet \mathcal{S} , the free-energy Γ of the system is written as

$$\Gamma(\mathbf{x}) = \iint_{\mathcal{S}} W(\mathbf{V}) dx dy - m_o \mathbf{g} \cdot \mathbf{p}_o, \quad (6)$$

where $\mathbf{V} \in \mathbb{R}^{2 \times 2}$ is the metric tensor of the deformed sheet. $W : SO(2) \rightarrow \mathbb{R}$ is the strain energy function, m_o is the mass of the object O , $\mathbf{g} = [0 \ 0 \ -g]^T$ and g is the gravitational constant. The strain energy function can be expressed as $W(\mathbf{V}) = \frac{E}{2} |\epsilon|^2$, $\epsilon = \sqrt{\mathbf{V}} - \mathbf{I}$ [2], where \mathbf{I} is the identity matrix, $E > 0$ is considered as elastic modulus of sheet \mathcal{S} and ϵ is the strain. Since \mathcal{S} is inelastic and flexible, $\mathbf{V} = \mathbf{I}$. Thus, $\Gamma(\mathbf{x})$ in (6) can be rewritten as

$$\Gamma(\mathbf{x}) = m_o g z_o \quad (7)$$

where z_o can be represented by \mathbf{x} by (3a).

The object always moves in the direction of the lowest potential energy and eventually comes to rest. The equilibrium position is determined and obtained by minimizing $\Gamma(\mathbf{x})$ with the linear geometric constraints (4). By observing (7), when $\Gamma(\mathbf{x})$ reaches its minimum, so does z_o . Therefore, by (3a), we construct an objective function $f(\mathbf{x})$ that is a quadratic real function.

$$f(\mathbf{x}) = -(z_r - z_o)^2 = (x_{i_1} - x_o)^2 + (y_{i_1} - y_o)^2 - (x_{vi_1} - x_{vo})^2 - (y_{vi_1} - y_{vo})^2 = \frac{1}{2} \mathbf{x}^T \mathbf{H} \mathbf{x} + \mathbf{c}^T \mathbf{x} + f_0, \quad (8)$$

where $0 < z_o < z_r$, $\mathbf{H} = \text{diag}(2, 2, -2, -2)$, $\mathbf{c} = [-2x_{i_1} - 2y_{i_1} \ 2x_{vi_1} \ 2y_{vi_1}]^T$, $f_0 = x_{i_1}^2 + y_{i_1}^2 - x_{vi_1}^2 - y_{vi_1}^2$. Thus, the solution of FK can be regarded as solving the following constrained quadratic problem (CQP).

$$\begin{aligned} \min_{\mathbf{x}} \quad & f(\mathbf{x}) = \frac{1}{2} \mathbf{x}^T \mathbf{H} \mathbf{x} + \mathbf{c}^T \mathbf{x} + f_0 \\ \text{s.t.} \quad & \mathbf{A}_1 \mathbf{x} = \mathbf{b}_1, \mathbf{A}_2 \mathbf{x} > \mathbf{b}_2, f(\mathbf{x}) < 0. \end{aligned} \quad (9)$$

For (9), we first use the Lagrangian multiplier method to solve \mathbf{x} and then bring the solution into the inequality to determine whether other conditions are satisfied. Before constructing Lagrangian function $L(\mathbf{x}, \lambda)$ and obtaining the non-singular Lagrangian matrix \mathbf{L} , we can find the maximum linearly independent equations in $\mathbf{A}_1 \mathbf{x} = \mathbf{b}_1$ by Gaussian elimination. Therefore, we further partition the equality constraint of (9) as

$$\mathbf{A}_1 = \begin{bmatrix} \mathbf{A}_{11} \\ \mathbf{A}_{12} \end{bmatrix}, \mathbf{b}_1 = \begin{bmatrix} \mathbf{b}_{11} \\ \mathbf{b}_{12} \end{bmatrix}, \mathbf{A}_{11} \mathbf{x} = \mathbf{b}_{11}, \mathbf{A}_{12} \mathbf{x} = \mathbf{b}_{12}, \quad (10)$$

where $\mathbf{A}_{11} \in \mathbb{R}^{(k_1-1) \times 4}$, $\mathbf{b}_{11} \in \mathbb{R}^{(k_1-1)}$, $\mathbf{A}_{12} \in \mathbb{R}^{(k-k_1) \times 4}$, $\mathbf{b}_{12} \in \mathbb{R}^{(k-k_1)}$, and $k_1 = \text{rank}(\mathbf{A}_1) + 1 \leq k$. $\mathbf{A}_{11} \mathbf{x} = \mathbf{b}_{11}$ is the maximum linearly independent equations. Therefore, \mathbf{A}_{11} is a row full rank matrix. Because of $\text{rank}(\mathbf{A}_{11}) \leq 4$, the value of k_1 can only be 3, 4, or 5. Fig. 3 shows an example of a 4-robot team to form a square shape. For such an example, $k = 4$, $k_1 = 3$, $\text{rank}(\mathbf{A}_{11}) = \text{rank}(\mathbf{A}_1) = 2$.

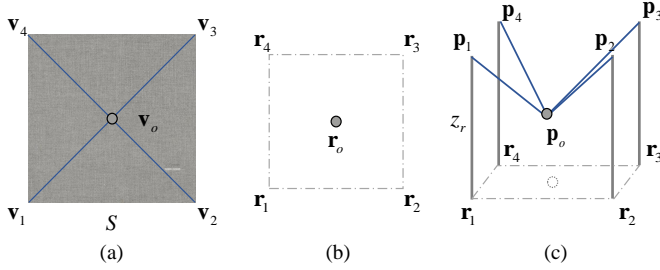


Fig. 3. A robot system that both the initial sheet shape and robot formation are square. The taut cable number is four, i.e., $k = 4$, but maximum linearly independent equations in $\mathbf{A}_1 \mathbf{x} = \mathbf{b}_1$ is $k_1 - 1 = 2$, that is, we only need to use the constraints of three taut cables ($k_1 = 3$).

After obtaining the maximum linearly independent equations, both $\mathbf{A}_{11} \mathbf{x} = \mathbf{b}_{11}$ and $\mathbf{A}_{12} \mathbf{x} = \mathbf{b}_{12}$ are satisfied. Therefore, the Lagrange function of (9) is defined as

$$L(\mathbf{x}, \boldsymbol{\lambda}) = \frac{1}{2} \mathbf{x}^T \mathbf{H} \mathbf{x} + \mathbf{c}^T \mathbf{x} - \boldsymbol{\lambda}^T (\mathbf{A}_{11} \mathbf{x} - \mathbf{b}_{11}), \quad (11)$$

where vector $\boldsymbol{\lambda} \in \mathbb{R}^{(k_1-1)}$. The optimal solution of $L(\mathbf{x}, \boldsymbol{\lambda})$ needs to satisfy the first-order conditions

$$\nabla_{\mathbf{x}} L(\mathbf{x}, \boldsymbol{\lambda}) = \mathbf{0}, \quad \nabla_{\boldsymbol{\lambda}} L(\mathbf{x}, \boldsymbol{\lambda}) = \mathbf{0}.$$

Then we obtain

$$\underbrace{\begin{bmatrix} \mathbf{H} & -\mathbf{A}_{11}^T \\ -\mathbf{A}_{11} & \mathbf{0} \end{bmatrix}}_{\mathbf{L}} \begin{bmatrix} \mathbf{x} \\ \boldsymbol{\lambda} \end{bmatrix} = \begin{bmatrix} -\mathbf{c} \\ -\mathbf{b}_{11} \end{bmatrix}, \quad (12)$$

where Lagrange matrix $\mathbf{L} \in \mathbb{R}^{(k_1+3) \times (k_1+3)}$. The solution of CQP (9) can be obtained by multiplying both sides of (12) with \mathbf{L}^{-1} provided the following fact.

Lemma 1: The Lagrange matrix \mathbf{L} in (12) is full rank and therefore invertible.

Proof 1: We need to prove that $\text{rank}(\mathbf{L}) = k_1 + 3$. We analyze the row rank of \mathbf{L} . Since $\text{rank}(\mathbf{H}) = 4$, the first four rows of \mathbf{L} are full rank. Therefore, \mathbf{L} is full rank if and only if $[-\mathbf{A}_{11} \quad \mathbf{0}]$ is row full rank, namely, $\text{rank}([- \mathbf{A}_{11} \quad \mathbf{0}]) = k_1 - 1$, which is true by definition of \mathbf{A}_{11} . Thus, $\text{rank}(\mathbf{A}_{11}) \equiv k_1 - 1$ and \mathbf{L} is invertible.

Indeed, the inverse matrix of \mathbf{L} is further obtained as follows.

$$\mathbf{L}^{-1} = \begin{bmatrix} \mathbf{H} & -\mathbf{A}_{11}^T \\ -\mathbf{A}_{11} & \mathbf{0} \end{bmatrix}^{-1} = \begin{bmatrix} \mathbf{B} & -\mathbf{C}^T \\ -\mathbf{C} & \mathbf{D} \end{bmatrix}, \quad (13)$$

where $\mathbf{B} = \mathbf{H}^{-1} - \mathbf{H}^{-1} \mathbf{A}_{11}^T (\mathbf{A}_{11} \mathbf{H}^{-1} \mathbf{A}_{11}^T)^{-1} \mathbf{A}_{11} \mathbf{H}^{-1}$, $\mathbf{C} = (\mathbf{A}_{11} \mathbf{H}^{-1} \mathbf{A}_{11}^T)^{-1} \mathbf{A}_{11} \mathbf{H}^{-1}$, $\mathbf{D} = -(\mathbf{A}_{11} \mathbf{H}^{-1} \mathbf{A}_{11}^T)^{-1}$. With (13) and (12), the solution of the \mathbf{x} is obtained as.

$$\mathbf{x} = -\mathbf{B} \mathbf{c} + \mathbf{C}^T \mathbf{b}_{11}, \quad \boldsymbol{\lambda} = \mathbf{C} \mathbf{c} - \mathbf{D} \mathbf{b}_{11}. \quad (14)$$

Since the maximum order of \mathbf{L} is 8, the computational complexity of obtaining solution is $O(1)$.

After obtaining \mathbf{x} , if $\mathbf{A}_2 \mathbf{x} > \mathbf{b}_2$, $f(\mathbf{x}) < 0$ also satisfies, $\bar{\mathbf{x}}$ is then the solution of CQP (9). z_o is obtained by (8) and due to $z_r > z_o$, z_o is expressed as

$$z_o = z_r - \sqrt{-f(\bar{\mathbf{x}})}, \quad (15)$$

where $z_o > 0$ needs to be satisfied; otherwise the object is in contact with the ground. By now, we can obtain the FK solution \mathbf{p}_o and \mathbf{v}_o when the taut cable set \mathcal{I}_t is given.

3) *Force Closure Condition:* The last step is to verify whether the solution obtained in the previous section is feasible physically. When k cables are taut, the force closure condition is given by

$$\sum_{i=1}^k F_i \boldsymbol{\tau}_i = -m_o \mathbf{g}, \quad (16)$$

where $F_i \geq 0$ is the magnitude of the tension force of the i th cable, $\boldsymbol{\tau}_i = \frac{\mathbf{p}_i - \mathbf{p}_o}{\|\mathbf{p}_i - \mathbf{p}_o\|}$ is the unit vector of the along the i th cable, $i \in \mathcal{I}_t$. The left side of (16) is the non-negative linear combination of $\boldsymbol{\tau}_i$, $i = 1, \dots, k$, which is known as the cone combination. $\boldsymbol{\tau}_i$ and all its cone combination form a convex cone \mathcal{C} with the origin at the object O . Condition (16) holds if and only if cone \mathcal{C} contains $-m_o \mathbf{g}$ [22]. Therefore, we get the criterion that if the projected point \mathbf{r}_o of object O on the XY plane is within the polygon formed by robots $\mathcal{R}_k = [\mathbf{r}_1 \dots \mathbf{r}_k]^T$ corresponding to the taut cables group \mathcal{I}_t , a set of F_i can be then found to satisfy (16). If this \mathcal{R}_k positioning condition is not satisfied force on the XY plane cannot be balanced.

B. Taut Cable Number Analysis

The geometric constraints of the taut cable set is $\mathbf{A}_1 \mathbf{x} = \mathbf{b}_1$, $\mathbf{A}_1 \in \mathbb{R}^{(k-1) \times 4}$ in (4). When $k \leq 5$, the number of equations is no more than or equals to four. Therefore, the system either has one solution or infinity solutions, while the form closure condition (5) is also satisfied. When $k > 5$, the number of equations is more than four and this leads to a no-solution situation. In this case, the form closure condition is difficult to satisfy. Therefore, the FK solution with more than five taut cables is rare but can exist, as shown in the results in the next section. We here present a special case with all cables taut as in the following lemma.

Lemma 2: For an N -robot system with a deformable sheet S , the robotic system has only one solution with all the virtual cables taut, where the robot formation is a regular N -side polygon. The contact point \mathbf{v}_o is at the center of S with the projected position \mathbf{r}_o of object O is at the center of the formation.

Proof 2: For a regular N -side polygon, we obtain that $\mathbf{v}_i = [r_s \cos \frac{2\pi i}{N} \quad r_s \sin \frac{2\pi i}{N}]^T$, $\mathbf{r}_i = [r_f \cos \frac{2\pi i}{N} \quad r_f \sin \frac{2\pi i}{N}]^T$, $i = 1, \dots, N$, where r_s and r_f are the radii of its circumscribed circles, respectively. According to (4), since $\mathbf{r}_i = \frac{r_f}{r_s} \mathbf{v}_i$, the third and fourth columns of \mathbf{A}_1 are eliminated by the elementary column transformation of the matrix. Thus, for any set of \mathcal{I}_t , we obtain $\mathbf{b}_1 = \mathbf{0}$, $\text{rank}(\mathbf{A}_1) = \text{rank}(\bar{\mathbf{A}}_1) = \text{rank}(\mathbf{A}_{11}) = 2$ and this implies $k_1 = 3$ for all k . By solving (9), we obtain $\mathbf{v}_o = \mathbf{0}$, $\mathbf{r}_o = \mathbf{0}$, $z_o = z_r - \sqrt{r_s^2 - r_f^2}$, $\mathcal{I}_t = \mathcal{I}_N$. Therefore, the object has a unique position with all taut virtual cables.

C. Forward Kinematics Algorithm

Section III-A presents how to solve the FK problem when the taut cable set \mathcal{I}_t is given. Algorithm 1 summarizes the

procedure to find all possible FK solutions. The algorithm searches all possible combinations of taut cables and then finds the possible solution. For an N -robot system, the minimum number of taut cables is $k \geq 3$ for stable equilibrium. Therefore, the total number of taut cable combinations is $\sum_{k=3}^N C_N^k$. Algorithm 1 consists of the following four main steps. *Step 1*: Select one \mathcal{I}_t with k taut cables from $\sum_{k=3}^N C_N^k$ combinations and this is achieved by function $\text{NChooseK}(N, k)$ (line 2). *Step 2*: Verify the form closure condition in (5) by function FormClosure (line 3). *Step 3*: Construct and solve the CQP to obtain $(\mathbf{p}_o, \mathbf{v}_o)$ by combining the form closure condition and minimum potential energy of the system (lines 4 and 5). *Step 4*: Verify the force closure condition and the cable tensions should be non-negative. If the condition is met, update sets \mathbb{P}_o , \mathbb{V}_o and \mathbb{I}_t and search for the next element in \mathcal{I}_t .

Algorithm 1: FK computation with VVCM

```

Input :  $N, z_r, \mathcal{V}_N^0, \mathcal{R}_N$ 
Output:  $\mathbb{P}_o, \mathbb{V}_o, \mathbb{I}_t$ .
1  $\mathbb{P}_o = \emptyset, \mathbb{V}_o = \emptyset, \mathbb{I}_t = \emptyset$ 
  if  $\text{FormationFeasible}(\mathcal{V}_N^0, \mathcal{R}_N)$  then
    for  $k = 3$  to  $N$  do
      for  $j = 1$  to  $C_N^k$  do
2          $\mathcal{I}_t = \text{NChooseK}(N, k)$  ;
3          $\text{FormClosure}(z_r, \mathcal{V}_N^0, \mathcal{R}_N, \mathcal{I}_t)$  ;
          if  $\text{rank}(\mathbf{A}_1) = \text{rank}(\bar{\mathbf{A}}_1)$  then
4             Obtain  $\mathbf{x}$  by (14) and  $z_o$  by (15) ;
5              $(\mathbf{v}_o, \mathbf{p}_o) \leftarrow (\mathbf{x}, z_o)$  ;
              if  $\text{ForceClosure}(\mathbf{v}_o, \mathbf{p}_o) = \text{True}$ 
                then
6                  $\mathbb{P}_o = \mathbb{P}_o \cup \mathbf{p}_o, \mathbb{V}_o = \mathbb{V}_o \cup \mathbf{v}_o,$ 
                   $\mathbb{I}_t = \mathbb{I}_t \cup \mathcal{I}_t$  ;
                end
              end
            end
          end
        end
      end
    end
  end
7 return False

```

Algorithm 1 traverses all taut cable sets to ensure the completeness of forward kinematics computation. The total number of loops of the algorithm is $\sum_{k=3}^N C_N^k$. We briefly discuss the computational complexity of each loop. After entering the loop, the worst time complexity of determining condition (5) is $O(k^2)$. If the form closure condition is satisfied, the complexity of constructing (10) is $O(k^2)$ and the calculation of CQP (14) is $O(1)$. Subsequently, the complexity of *Step 4* is $O(k)$. Therefore, the total complexity of each loop is $O(k^2)$. By the above analysis, the main contribution of complexity is the number of combinations (loops). Fortunately, if the condition (5) is satisfied, the CQP does not have a feasible solution and then a new loop search starts. Therefore, the algorithm can complete all combination searches fast and we will analyze the improvement of algorithm efficiency based on simulation examples in the next section.

IV. EXPERIMENTAL AND SIMULATION RESULTS

A. Experimental Setup

We conduct physical and simulation experiments to verify and demonstrate the effectiveness of Algorithm 1. We constructed a four-robot team in experiments, as shown in Fig. 1(a). To satisfy the VVCM conditions and help build an experimental platform, we chose a solid metal ball (radius 25 mm) as the handling object. A soft plastic cloth was selected as shown in Fig. 1(b), and \mathcal{V}_N^0 is listed in Fig. 4. A rod was mounted on each robot and the deformable sheet was held on the tip of the rod. The height of holding points was $z_r = 0.8$ m in the experiment. The elastic deformation of the sheet during the experiment can be ignored. The position of the holding points and the object were measured by the motion capture system (6 cameras from NOKOV) at a rate of 60 Hz. The robot was a differential wheel structure driven by two stepper motors with an embedded system (Arduino UNO R3). The communication method between robots was ZigBee, which is a wireless network protocol for low-speed and short-distance transmission.

B. Experimental and Simulation Results

Given the robot formation, Algorithm 1 calculated all feasible equilibrium states, each of which was constrained by the corresponding taut cable group \mathcal{I}_t . We took a four-robot team as Example 1 to verify the effectiveness of the proposed FK method. Fig 4 shows the experimental and simulation results of different combinations of taut cable sets for the 4-robot team. The positions of the robots \mathcal{R}_N and vertex positions \mathcal{V}_N^0 are shown in the figure. There are three FK solutions for this example, as shown in Fig. 4. The top row in the figure is the simulation results, and the bottom row is the corresponding experimental results.

Table I lists the experimental results and the comparison with the simulation results. The errors are mainly caused by position errors of the markers, whose diameter is 1 cm. Most of the errors are within 1 cm. The large errors on the X and Y axes in Fig. 4(c) are 6.43% and 15.13%, respectively. This is because, among all three solutions of the example, the height of the object z_o in Fig. 4(a) and 4(b) was lower than that in Fig. 4(c) and therefore, the potential energy in the former case was lower than that in the latter case and the equilibrium state is more stable. There was a tendency of the object to roll towards the other two FK solutions and this resulted in large error.

We then conducted simulation results with to illustrate the FK algorithm and solution analysis. An eight-robot team ($N = 8$) was selected as Example 2 to verify the FK completeness. The height of the held object was set to 1 m. The shape of the sheet was selected as a regular octagon, and the radius of its circumscribed circle was $r_s = 0.9$ m. Fig. 5 shows the results of \mathcal{R}_N and \mathcal{V}_N^0 . Similar to the previous example, the FK algorithm found all feasible equilibrium states and Table II lists the number of valid \mathcal{I}_t after each step of the algorithm. The last column indicates whether the step produced a solution after computation.

TABLE I
EXPERIMENT RESULTS AND ERRORS OF FORWARD KINEMATICS SOLUTIONS FOR THE FOUR-ROBOT TEAM
($N = 4$, $z_r = 0.8$ M, $Error = \frac{\|p_o^{real} - p_o^{sim}\|}{\|p_o\|^{sim}} \times 100\%$)

Taut cable set \mathcal{I}_t	p_o (m)			Taut Cable Length (m)			
	x_o	y_o	z_o	No. 1	No. 2	No. 3	No. 4
{1, 2, 3}	0.571 (0.36%)	0.320 (-1.44%)	0.143 (4.62%)	0.773 (-0.72%)	0.753 (-1.04%)	0.772 (-0.63%)	–
{1, 3, 4}	0.566 (1.36%)	0.341 (-0.05%)	0.144 (4.98%)	0.776 (-0.32%)	–	0.767 (-1.18%)	0.766 (-0.59%)
{1, 2, 3, 4}	0.463 (6.43%)	0.275 (15.13%)	0.158 (4.56%)	0.706 (1.43%)	0.766 (-1.08%)	0.827 (-3.83%)	0.779 (-3.26%)

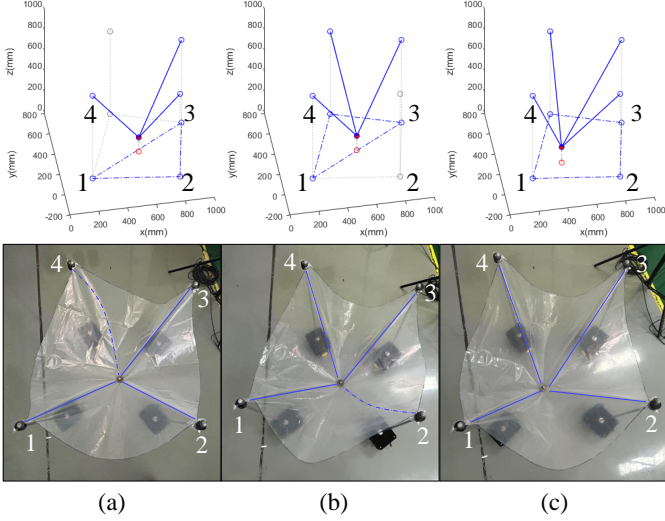


Fig. 4. The forward kinematics simulation (top row) and experimental results (bottom row) of four-robot formation to handle an object with a deformable sheet. $\mathcal{V}_N^0 = [-0.32 \ -0.42; 0.80 \ -0.38; 0.75 \ 0.71; -0.37 \ 0.66]^T$ m, and $\mathcal{R}_N = [0.21 \ 0.12; 0.80 \ 0.04; 0.90 \ 0.55; 0.44 \ 0.72]^T$ m. A straight line segment (taut cable) is formed when the plastic sheet is subjected to tension, which is marked by a blue solid line. (a) $\mathcal{I}_t = \{1, 2, 3\}$. (b) $\mathcal{I}_t = \{1, 3, 4\}$. (c) $\mathcal{I}_t = \{1, 2, 3, 4\}$.

TABLE II
THE VALID \mathcal{I}_k AFTER EACH STEP OF ALGORITHM 1 IN EXAMPLE 2

Step	Conditions to be met	Element number $k = \mathcal{I}_k $	(p_o, v_o)
1	All taut cable combinations	219 (100%)	×
2	Form closure feasible	182 (83.11%)	×
3	CQP feasible	22 (10.05%)	✓
4	Force closure feasible	6 (2.74%)	✓

From the results in Table II, we observe that there are 219 combinations of possible taut cables sets in \mathbb{I}_t of the eight-robot system. Out of these sets, 37 combinations did not meet the form closure condition (5) and were then eliminated. In Step 3 of the algorithm, we computed and obtained solution x and these solutions still need to satisfy the constraints that the rest of the cables are slack ($A_2 x > b_2$) and the height of the object is feasible, $z_o \in (0, z_r)$. Therefore, after solving the CQP, only 22 solutions (p_o, v_o) were feasible out of the 182 solutions. Finally, we verified the force closure condition of these 22 solutions and obtained the following six FK solutions.

We list all FK solutions $\{p_o, v_o\}$ and their taut cables group \mathcal{I}_t in Table III.

TABLE III
FK SOLUTIONS AND RESULTS FOR EXAMPLE 2

Taut Cable Group \mathcal{I}_t	v_o (mm)		p_o (mm)		
	x_{vo}	y_{vo}	x_o	y_o	z_o
{4, 5, 8}	-12.7	-13.0	-8.6	-30.5	261.8
{1, 5, 7, 8}	-14.8	-193.2	-26.6	-347.8	310.2
{3, 4, 5, 8}	16.4	-22.2	43.3	-46.9	263.2
{3, 5, 7, 8}	51.4	-165.0	98.7	-290.9	300.5
{4, 5, 6, 8}	-220.7	-76.7	-389.3	-142.0	340.6
{1, 3, 5, 7, 8}	-13.9	-193.3	-25.0	-348.0	310.2

Out of these six solutions, one solution is with three taut cables, four solutions are with four taut cables, and one solution is with five taut cables. Fig. 5 shows the robot formation and positions of these results, which demonstrates six equilibrium states under the same robot formation. It is interesting to observe that both Fig. 5(c) and 5(e) contain the taut cable set {4, 5, 8}, which is also the taut cables in Fig. 5(a). These three solutions are different because of various A_{11} and b_{11} in (14) for given different taut cable sets. Same observation is obtained from three solutions in Fig. 5(b), 5(d), and 5(f), in which the taut cable sets all contain {5, 7, 8}. Among all six solutions, the results in Fig. 5(a) and 5(c) are with the lowest potential energy.

For Example 2, as shown in Table II, each step in the FK algorithm significantly reduces the number of possible solutions that were obtained in the previous step (i.e., third column of the table). To further verify the efficiency improvement of the FK algorithm, we conducted a simulation of three examples with robot numbers $N = 10, 15$, and 20 , marked as Examples 3, 4, and 5, respectively. Table IV lists the initial sheet shape \mathcal{V}_N^0 , robot formation \mathcal{R}_N , and the proportion of infeasible combinations computed in Step 2. The computed reduction rate in Step 2 is listed in the fourth column in the table, that is, 39.%, 85.2%, and 98.0% for $N = 10, 15, 20$, respectively. It is found that as the number of robots increases, Step 2 significantly reduces the complexity of the algorithm and improves its efficiency.

The previous examples show that even for the cases where the number of robots $N > 5$, the taut cable number of the FK solutions is less than five, which confirms the taut cable number analysis in Section III-B. For the equilibrium state with more than five taut cables, we took and simulated

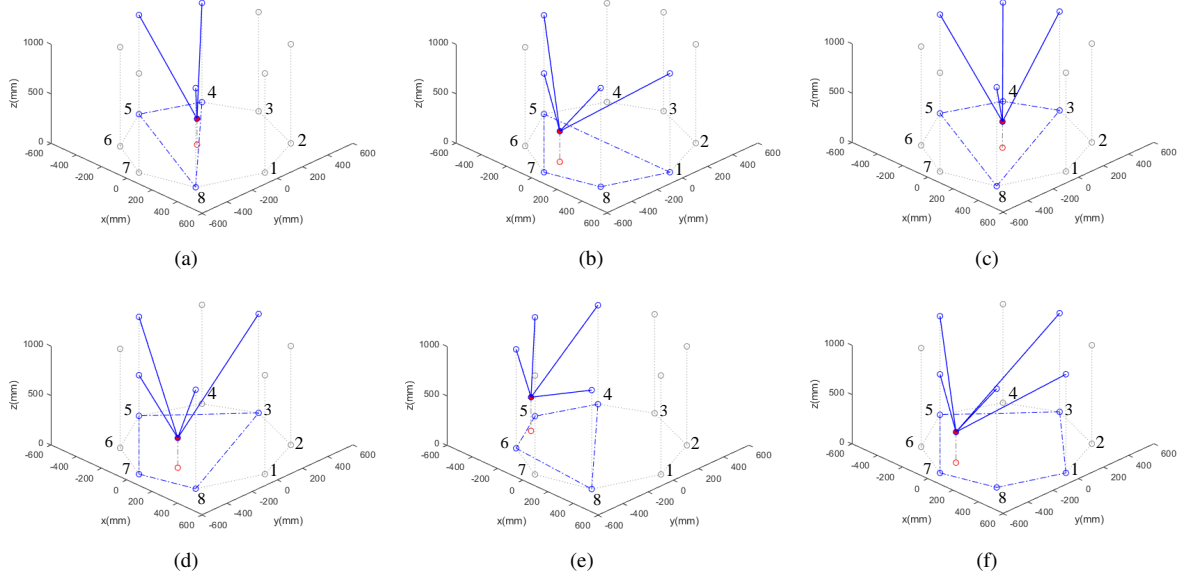


Fig. 5. Forward kinematics computation for an eight-robot formation of Example 2. The solid blue line represents the taut cable and the red solid point represents the object O . The blue dotted line indicates the sub-formation of the robots involved in the handling the object. The sheet shape is a regular octagon, and the radius of its circumscribed circle is 0.9 m. $\mathcal{R}_N = [0.5 \ 0; 0.35 \ 0.35; -0.05 \ 0.5; -0.35 \ 0.35; -0.50 \ 0; -0.30 \ -0.35; 0 \ -0.50; 0.35 \ -0.40]^T$ m. (a) $\mathcal{I}_t = \{4, 5, 8\}$. (b) $\mathcal{I}_t = \{1, 5, 7, 8\}$. (c) $\mathcal{I}_t = \{3, 4, 5, 8\}$. (d) $\mathcal{I}_t = \{3, 5, 7, 8\}$. (e) $\mathcal{I}_t = \{4, 5, 6, 8\}$. (f) $\mathcal{I}_t = \{1, 3, 5, 7, 8\}$.

TABLE IV
FK COMPUTATION AND RESULTS OF THREE MULTI-ROBOT SYSTEMS ($N = 10, 15, 20$)

Robot number N	Taut cable set (Step 1), M_1	Form closure feasible (Step 2), M_2	Reduction rate $\frac{M_1 - M_2}{M_1}$	CQP feasible (Step 3), M_3	Force closure feasible (Step 4), $M_4 = M$	Taut cable number		
						$k = 3$	$k = 4$	$k = 5$
10 ⁽¹⁾	968	582	39.9%	34	5	0	2	3
15 ⁽²⁾	32,647	4,823	85.2%	93	2	1	1	0
20 ⁽³⁾	1,048,365	21,489	98.0%	152	13	1	6	6

- ⁽¹⁾ Example 3: $\mathcal{V}_N^0 = [27 \ 7; 54 \ 2; 85 \ 7; 98 \ 36; 96 \ 65; 76 \ 93; 44 \ 96; 15 \ 75; 7 \ 48; 12 \ 22]^T$ cm, $\mathcal{R}_N = [45 \ 14; 64 \ 14; 80 \ 27; 81 \ 47; 78 \ 64; 66 \ 76; 49 \ 78; 33 \ 66; 27 \ 43; 30 \ 23]^T$ cm.
⁽²⁾ Example 4: $\mathcal{V}_N^0 = [50 \ 4; 65 \ 5; 80 \ 12; 91 \ 24; 94 \ 43; 91 \ 63; 80 \ 80; 65 \ 91; 46 \ 94; 28 \ 84; 15 \ 69; 11 \ 51; 11 \ 30; 18 \ 10; 33 \ 3]^T$ cm, $\mathcal{R}_N = [2 \ 13; 64 \ 15; 72 \ 21; 77 \ 32; 79 \ 47; 76 \ 59; 68 \ 67; 59 \ 72; 48 \ 73; 37 \ 66; 30 \ 55; 26 \ 42; 26 \ 30; 29 \ 19; 40 \ 12]^T$ cm.
⁽³⁾ Example 5: $\mathcal{V}_N^0 = [51 \ 6; 62 \ 6; 73 \ 9; 82 \ 15; 88 \ 25; 92 \ 39; 93 \ 53; 91 \ 67; 85 \ 80; 77 \ 89; 67 \ 95; 56 \ 97; 45 \ 94; 35 \ 88; 27 \ 78; 20 \ 62; 19 \ 47; 21 \ 33; 27 \ 20; 38 \ 11]^T$ cm, $\mathcal{R}_N = [58 \ 16; 64 \ 18; 68 \ 23; 72 \ 29; 74 \ 36; 77 \ 45; 77 \ 54; 75 \ 65; 71 \ 71; 66 \ 75; 60 \ 77; 55 \ 77; 50 \ 73; 46 \ 64; 46 \ 55; 47 \ 46; 48 \ 37; 50 \ 30; 52 \ 24; 54 \ 19]^T$ cm.

TABLE V
FK SOLUTIONS WITH MORE THAN FIVE TAUT CABLES IN EXAMPLE 6 ($N = 8$, $z_r = 1$ m, $r_s = 0.9$ m, $r_f = 0.5$ m)

Formation change $\delta = [50 \ 0]^T$ mm	Taut cable number k	Taut cable set \mathcal{I}_t	$\text{rank}(\mathcal{A}_1)$	FK number M	\mathbf{v}_o (m)		\mathbf{p}_o (m)		
					x_{vo}	y_{vo}	x_o	y_o	z_o
(a) —	8	$\{1, 2, 3, 4, 5, 6, 7, 8\}$	2	1	0	0	0	0	0.252
(b) $\mathbf{r}_1 = \mathbf{r}_1 - \delta$	7	$\{2, 3, 4, 5, 6, 7, 8\}$	2	1	0	0	0	0	0.252
(c) $\mathbf{r}_1 = \mathbf{r}_1 - \delta, \mathbf{r}_5 = \mathbf{r}_5 + \delta$	6	$\{2, 3, 4, 6, 7, 8\}$	2	1	0	0	0	0	0.252

the 8-robot system with the regular octagonal sheet, marked as Example 6. The initial shape of the sheet was the same as that of Example 2. We first show the special case given in Lemma 2 and then we fine-tuned the shape of regular polygonal formation by changing the position of the robots to construct the equilibria with more than five taut cables. Fig. 6 shows the simulation results of the robot formation and active cable sets and Table V further lists the detailed computational results. The results show three cases with more than five

taut cables in robot formation, that is, $k = 8, 7, 6$. Fig. 6(b) and 6(c) show the robot formations that were perturbed with a small range (marked as δ in the table) from the formation in Fig. 6(a). It is interesting to notice that the position of the object O remains unchanged in these three cases, which shows that the special case discussed in Lemma 2 is stable. Under this formation, a unique and stable solution to the FK problem is particularly of interest that would be useful for object manipulation and transportation tasks.

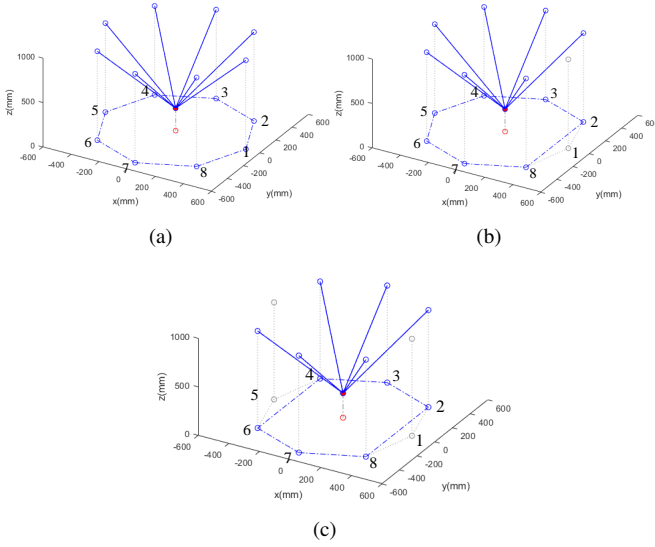


Fig. 6. Simulation results of three cases in Example 6 where the number of taut cables is greater than 5. \mathcal{V}_N^0 is the same as that in Example 2. (a) $\mathcal{I}_t = \{1, 2, 3, 4, 5, 6, 7, 8\}$. The robot position is $\mathbf{r}_i = [r_f \cos \frac{2\pi(i-1)}{N}, r_f \sin \frac{2\pi(i-1)}{N}]^T$ m, $i = 1, \dots, N$, $r_f = 0.5$ m. (b) $\mathcal{I}_t = \{2, 3, 4, 5, 6, 7, 8\}$. (c) $\mathcal{I}_t = \{2, 3, 4, 6, 7, 8\}$.

The FK algorithm finds all equilibrium states under which the object might have different potential energies and therefore stability. It was further discovered in the experiment that the equilibrium state position with high potential energy tended to move close toward the position with lower potential energy. This implies that equilibrium states with lower potential energy are more stable and more suitable for transporting tasks. Further study should look into this observation and further develop motion control and planning strategies for the robotic team.

V. CONCLUSION

In this paper, we extended the concept of virtual variable cable model and (VVCM) and presented a complete forward kinematics method for multi-robot-based object handling and transport with a deformable sheet. Users can choose the arbitrarily number and formation of robots, the heights of handling point of the deformable sheet, and the shape of sheet as the inputs of the forward kinematics algorithm to obtain the feasible object positions in the world and sheet frames. The forward kinematics algorithm was built on a set of geometric and physical constraints and can efficiently compute the object position for possible real-time robot planning and control. Through the simulation and experiment, we demonstrated the effectiveness, completeness, efficiency of the FK method with variations of robot numbers and formation. The future developments include consideration of dynamic effects of the object motion and disturbances during the handling and transporting process. Using the proposed FK method and algorithm for robot motion planning and control is also among the ongoing research directions.

REFERENCES

- [1] B. Roy, A. Basnajian, and H. H. Asada, "Repositioning of a rigid body with a flexible sheet and its application to an automated rehabilitation bed," *IEEE Trans. Automat. Sci. Eng.*, vol. 2, no. 3, pp. 300–307, 2005.
- [2] K. Hunte and J. Yi, "Collaborative object manipulation through indirect control of a deformable sheet by a mobile robotic team," in *Proc. IEEE Conf. Automat. Sci. Eng.*, Vancouver, Canada, 2019, pp. 1463–1468.
- [3] Y. Bai, W. Yu, and C. K. Liu, "Dexterous manipulation of cloth," in *Comp. Graph. Forum*, vol. 35, no. 2, 2016, pp. 523–532.
- [4] J. Zhu, A. Cherubini, C. Dune, D. Navarro-Alarcon, F. Alambeigi, D. Berenson, F. Ficuciello, K. Harada, J. Kober, X. Li *et al.*, "Challenges and outlook in robotic manipulation of deformable objects," *IEEE Robot. Automat. Mag.*, vol. 29, no. 3, pp. 67–77, 2022.
- [5] D. McConachie, A. Dobson, M. Ruan, and D. Berenson, "Manipulating deformable objects by interleaving prediction, planning, and control," *Int. J. Robot. Res.*, vol. 39, no. 8, pp. 957–982, 2020.
- [6] R. Herguedas, G. López-Nicolás, R. Aragüés, and C. Sagüés, "Survey on multi-robot manipulation of deformable objects," in *Proc. IEEE Int. Conf. Emerg. Technol. Factory Automat.*, 2019, pp. 977–984.
- [7] K. Hunte and J. Yi, "Collaborative manipulation of spherical-shape objects with a deformable sheet held by a mobile robotic team," *IFAC-PapersOnLine*, vol. 54, no. 20, pp. 437–442, 2021.
- [8] —, "Pose control of a spherical object held by deformable sheet with multiple robots," *IFAC-PapersOnLine*, vol. 55, no. 37, pp. 414–419, 2022.
- [9] A. Capua, A. Shapiro, and S. Shoval, "Spiderbot: a cable suspended mobile robot," in *Proc. IEEE Int. Conf. Robot. Autom.*, Shanghai, China, 2011, pp. 3437–3438.
- [10] J. Hu, W. Liu, H. Zhang, J. Yi, and Z. Xiong, "Multi-robot object transport motion planning with a deformable sheet," *IEEE Robot. Automat. Lett.*, vol. 7, no. 4, pp. 9350–9357, 2022.
- [11] A. Capua, A. Shapiro, and S. Shoval, "Motion analysis of an underconstrained cable suspended mobile robot," in *Proc. IEEE Int. Conf. Robot. Biomimet.*, Guilin, China, 2009, pp. 788–793.
- [12] S.-R. Oh and S. K. Agrawal, "Cable suspended planar robots with redundant cables: Controllers with positive tensions," *IEEE Trans. Robotics*, vol. 21, no. 3, pp. 457–465, 2005.
- [13] S. Qian, B. Zi, W.-W. Shang, and Q.-S. Xu, "A review on cable-driven parallel robots," *Chinese J. Mech. Eng.*, vol. 31, no. 1, pp. 1–11, 2018.
- [14] M. Carricato and J.-P. Merlet, "Stability analysis of underconstrained cable-driven parallel robots," *IEEE Trans. Robotics*, vol. 29, no. 1, pp. 288–296, 2012.
- [15] A. Pott, "An algorithm for real-time forward kinematics of cable-driven parallel robots," in *Advances Robot Kinematics: Motion in Man and Machine*, J. Lenarcic and M. M. Stanisic, Eds., 2010, pp. 529–538.
- [16] H. An, H. Yuan, K. Tang, W. Xu, and X. Wang, "A novel cable-driven parallel robot with movable anchor points capable for obstacle environments," *IEEE/ASME Trans. Mechatronics*, vol. 27, no. 6, pp. 5472–5483, 2022.
- [17] J.-P. Merlet, "Maximal cable tensions of a n-1 cable-driven parallel robot with elastic or ideal cables," in *Int. Conf. Cable-Driven Paralle. Robots*, 2021, pp. 79–89.
- [18] J.-F. Collard and P. Cardou, "Computing the lowest equilibrium pose of a cable-suspended rigid body," *Optim. Eng.*, vol. 14, pp. 457–476, 2013.
- [19] X. Diao and O. Ma, "A method of verifying force-closure condition for general cable manipulators with seven cables," *Mech. Mach. Theory*, vol. 42, no. 12, pp. 1563–1576, 2007.
- [20] C. B. Pham, S. H. Yeo, G. Yang, M. S. Kurbanhusen, and I.-M. Chen, "Force-closure workspace analysis of cable-driven parallel mechanisms," *Mech. Mach. Theory*, vol. 41, no. 1, pp. 53–69, 2006.
- [21] R. Fletcher, *Practical Methods of Optimization*. John Wiley & Sons, 2000.
- [22] W. Fenchel, *Convex Cones, Sets, and Functions*. Department of Mathematics, Princeton University, 1953.